

Investigation of high $\Delta\epsilon$ derivatives of the [closo-1-CB₉H₁₀][−] anion for liquid crystal display applications†Jacek Pecyna,^a Piotr Kaszyński,^{*ab} Bryan Ringstrand^a and Matthias Bremer^cCite this: *J. Mater. Chem. C*, 2014, 2, 2956Received 4th February 2014
Accepted 4th March 2014

DOI: 10.1039/c4tc00230j

www.rsc.org/MaterialsC

Introduction

Polar liquid crystals and polar compounds compatible with nematic materials are important for adjusting dielectric anisotropy, $\Delta\epsilon$, and hence modifying electrooptical properties of materials used in liquid crystal display (LCD) technology.^{1,2} In this context, we have been investigating zwitterionic derivatives of the [closo-1-CB₉H₁₀][−] cluster (**A**, Fig. 1) as potential additives to liquid crystalline hosts. Recently, we demonstrated that polar derivatives, **1[6]**, **2[n]** and **3[6]a** (Chart 1), of type **IA** (Fig. 1) significantly increase $\Delta\epsilon$ of a nematic host and have high virtual N–I transitions, $[T_{NI}]$, although they themselves rarely are mesogenic.^{3,4} Unfortunately, these compounds have limited solubility in nematic materials, and their high $\Delta\epsilon$ values were extrapolated from infinite dilutions. Subsequent investigation of zwitterionic esters of type **IIA** (Fig. 1), containing a sulfonium group (**4[5]a** and **4[5]b**, Chart 1) or a pyridinium fragment (**5**,^{5,6} Chart 1) revealed that they form nematic phases, have satisfactory solubility in nematic hosts, and possess $\Delta\epsilon$ between 30 and 40. For the 4-cyanophenol ester in series 5 a record high $\Delta\epsilon$ of 113 was measured in a nematic host.^{5,6}

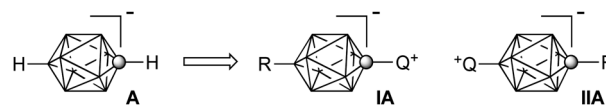


Fig. 1 The structure of the [closo-1-CB₉H₁₀][−] cluster (**A**) and its polar derivatives **IA** and **IIA**. Each vertex represents a BH fragment, the sphere is a carbon atom, and Q⁺ stands for an onium group such as an ammonium, sulfonium or pyridinium.

In continuation of our search for new polar compounds with improved mesogenic and dielectric properties, we investigated derivatives **3[n]** and esters **4[n]** (Chart 1). Here, we report the synthesis and thermal and dielectric characterization of the two series of compounds in the pure form as well as in binary mixtures. Dielectric data is analyzed with the Maier–Meier relationship and augmented with DFT computational results.

Results

Synthesis

Compounds **3[3]b**, **3[5]b**, and **3[6]c** were prepared by Negishi coupling of the appropriate organozinc reagent with iodide **6** (ref. 7) in the presence of Pd₂dba₃ and [HPCy₃]⁺[BF₄][−] in a THF–NMP mixture (Scheme 1).³ The iodides **6** were obtained from protected mercaptans **7** (ref. 3) upon reactions with an appropriate dibromides **8** (ref. 7) under hydrolytic conditions as described before.³

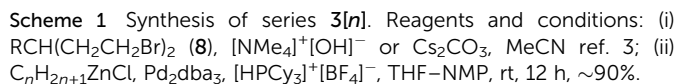
Aromatic esters **4[n]a–4[n]l** were prepared by reacting acid chlorides of sulfonium acids **9[n]** with appropriate phenols **10** in the presence of NEt₃ (Scheme 2). The two aliphatic esters,

^aDepartment of Chemistry, Vanderbilt University, Nashville, TN 37235, USA. E-mail: piotr.kaszyński@vanderbilt.edu; Tel: +1-615-322-3458

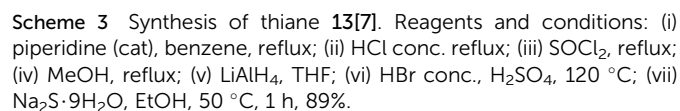
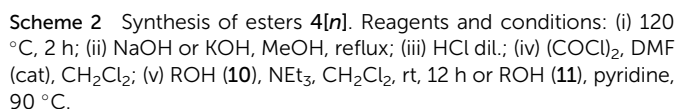
^bFaculty of Chemistry, University of Łódź, Tamka 12, 91403 Łódź, Poland

^cMerck KGaA, Frankfurter Strasse 250, Darmstadt, Germany

† Electronic supplementary information (ESI) available: Additional synthetic and characterization details for **3[n]**, **4[n]**, **8[7]**, **9[7]**, **10**, **11**, **13–19**, solubility data, thermal and dielectric data for solutions, Maier–Meier analysis details, DFT results, and archive of calculated equilibrium geometries for **3[n]**, **4[n]** and **20**. See DOI: 10.1039/c4tc00230j



Thiane 13[7] was prepared in reaction of dibromide 8[7] with Na₂S in EtOH-H₂O (Scheme 3).⁸ Dibromide 8[7] (ref. 10) was obtained following a previously established procedure for dibromide 8[5].⁷ Thus, octanal and dimethyl malonate were

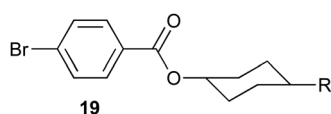


converted to dimethyl 3-heptylglutarate (**15**[7]) in 4 steps and 65% overall yield (Scheme 3). Subsequently, the ester was reduced to diol **16**[7] and converted to dibromide **8**[7].

Phenols **10j** and **10k** were prepared from the corresponding 4-benzyloxybenzoic acids **17**. The acids were converted into esters **18** after which the protecting benzyl group was removed under reductive conditions (Scheme 4).

Phenol **10g** (ref. 11) was obtained using a ligand-free Suzuki coupling reaction¹² (Scheme 5). Phenols **10h**,¹³ **10i**,^{14,15} and **10l** (ref. 16) were obtained as reported in the literature.

trans-4-Alkylcyclohexanols **11** (ref. 17) were isolated as **19** from a mixture of stereoisomers by recrystallization of their 4-bromobenzoate esters followed by hydrolysis.

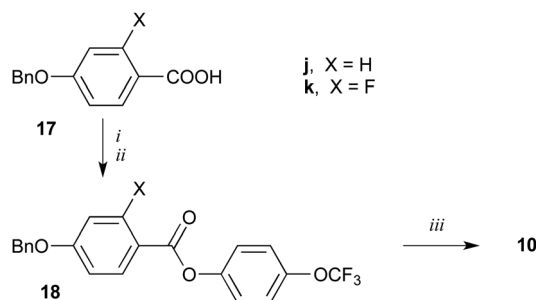


Thermal analysis

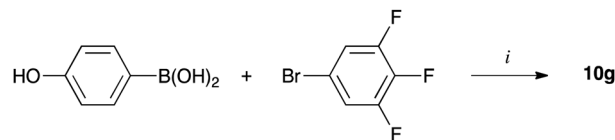
Transition temperatures and enthalpies of compounds **3**[*n*] and **4**[*n*] were determined by differential scanning calorimetry (DSC). Phase structures were assigned by optical microscopy in polarized light, and the results are shown in Tables 1–3.

Compounds in series **3**[*n*] display only crystalline polymorphism and melt at or above 200 °C, which is consistent with behavior of the previously reported derivative **3**[**6**]**a**.³ Extension of the sulfonium substituent in **3**[**6**]**a** by the cyclohexylethyl fragment in **3**[**6**]**c** increased the melting point by 44 K. Analogous comparison of **3**[**3**]**b** and **3**[**5**]**b** shows that extension of the alkyl group at the B(10) position by two methylene groups lowered the melting point by 25 K. Thus, in contrary to expectations, elongation of the core in **3**[**6**]**a** did not induce mesogenic behavior or reduce the melting point.

Esters in series **4**[**3**] generally have lower melting points than compounds in series **3**[*n*] and some exhibit nematic behavior. Among the single-ring phenol and alcohol derivatives, **4**[**3**]**b**–**4**[**3**]**f**, only the 4-butoxyphenol ester **4**[**3**]**b** displays a monotropic nematic phase and has the lowest melting point in the entire series (111 °C, Table 2). Extension of the phenol core by another ring generally increases the melting point, and also induces nematic behavior. The only exception is the



Scheme 4 Synthesis of phenols **10j** and **10k**. Reagents and conditions: (i) (COCl)₂, DMF (cat), CH₂Cl₂; (ii) 4-HOC₆H₄OCF₃, NEt₃, CH₂Cl₂; (iii) H₂, Pd/C, EtOH/THF or AcOEt/EtOH, rt, 12 h, >90%.



Scheme 5 Synthesis of phenol **10g**. Reagents and conditions: (i) PdCl₂, K₂CO₃, EtOH–H₂O (1 : 1), rt, 1 h, 79%.

Table 1 Transition temperatures (°C) and enthalpies (kJ mol^{−1}, in italics) for **3**[*n*]^a

		n	R	Transition temperatures and enthalpies
3	b		Cr ₁ 185 (3.0) Cr ₂ 224 (20.5) I	
5	b		Cr ₁ 189 (5.2) Cr ₂ 199 (13.9) I	
6	a	–CH ₂ CH ₃	Cr ₁ ^b 66 (21.9) Cr ₂ 209 (10.9) I ^c	
6	c		Cr ₁ 230 (9.8) Cr ₂ 253 (11.6) I	

^a Determined by DSC (5 K min⁻¹) on heating: Cr – crystal, N – nematic, I – isotropic. ^b Additional Cr–Cr transition at 133 °C (14.6). ^c Ref. 3.

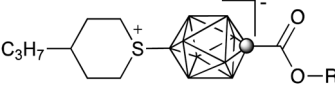
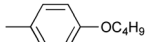
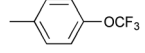
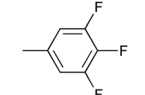


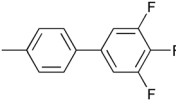
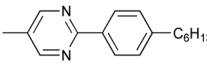
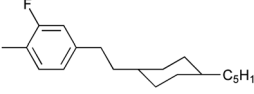
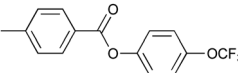
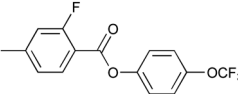
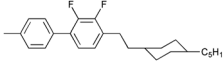
^a Determined by DSC (5 K min^{−1}) on heating: Cr – crystal, N – nematic, I – isotropic. ^b Additional Cr–Cr transition at 133 °C (14.6). ^c Ref. 3.

3,4,5-trifluorophenol derivative **4**[**3**]**d**, in which the addition of the benzene ring does increase the melting point by 85 K in **4**[**3**]**g** but fails to induce a mesophase. However, another biaryl derivative, phenylpyrimidinol ester **4**[**3**]**h** with a terminal hexyl group, does exhibit a 44 K wide nematic phase. Insertion of a –C₆H₄COO– fragment into the 4-trifluoromethoxyphenyl ester **4**[**3**]**c** only moderately increases the melting point (by 25 K) in **4**[**3**]**j** and induces a wide-range enantiotropic nematic phase (*T*_{NI} = 244 °C) along with rich crystalline polymorphism. Substitution of a lateral fluorine into the benzoate fragment of **4**[**3**]**j** lowered the nematic phase stability by 10 K, and, contrary to expectations, markedly increased the melting temperature in **4**[**3**]**k**. Finally, insertion of a fluorophenylethyl fragment into the cyclohexyl ester **4**[**3**]**f** increased the melting point by 38 K and induced a 26 K wide nematic phase in **4**[**3**]**i**. Similar insertion of a fluorinated biphenylethyl fragment into **4**[**3**]**f** resulted in appearance of a nematic phase in **4**[**3**]**l** (*T*_{NI} = 278 °C).

The effect of alkyl chain extension at the thiane ring on thermal properties was investigated for select esters **4**[**3**] (Table 3). Thus, extending the C₃H₇ chain in **4**[**3**]**b** to C₅H₁₁ in **4**[**5**]**b** lowered the melting point by 10 K, and had no impact on nematic phase stability. Further extension of the terminal chain to C₇H₁₅ lowered *T*_{NI} by 4 K in **4**[**7**]**b**. The same alkyl chain extension in the phenylpyrimidinol ester **4**[**3**]**h** had little effect on the melting temperature, however, it lowered *T*_{NI} by 10 K in the pentyl analogue **4**[**5**]**h** and by an additional 22 K in the heptyl derivative **4**[**7**]**h**. More significant melting point reduction, by about 25 K, is observed in derivatives **4**[**3**]**c** and **4**[**3**]**j**



Table 2 Transition temperatures (°C) and enthalpies (kJ mol⁻¹, in italics) for **4[3]**^a

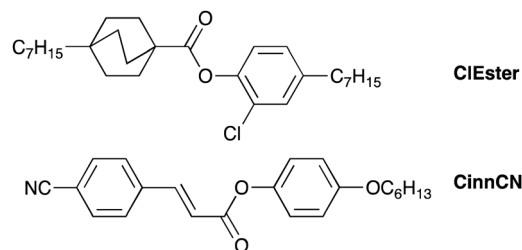
		
R		
b		Cr 111 (29.3) (N 96 (1.1)) I ^b [N 19] ^c
c		Cr 135 (31.6) I
d		Cr ₁ 102 (6.3) Cr ₂ 140 (21.0) I [N -34] ^e [N 21] ^d
e		Cr ₁ 140 (3.2) Cr ₂ 158 (19.9) I [N -1] ^c [N -4] ^d
f		Cr ₁ 101 (2.6) Cr ₂ 137 (15.7) I
g		Cr 225 (40.8) I
h		Cr 187 (36.4) N 231 (0.7) I [N 161] ^d
i		Cr 175 (27.7) N 201 (3.8) I
j		Cr ^e 160 (23.7) N 244 (1.3) I
k		Cr ^f 183 (29.9) N 234 (1.7) I
l		Cr 183 (36.1) N 278 (1.5) I [N 331] ^d

^a Determined by DSC (5 K min⁻¹) on heating; Cr – crystal, N – nematic, I – isotropic. ^b Ref. 8. ^c Virtual [T_{NI}] obtained in **CinnCN** typical error about ±5 K. ^d Virtual [T_{NI}] obtained in **ClEster** typical error about ±2 K. ^e Cr–Cr transition at 137 °C (27.6); another crystalline polymorph melts at 165 °C. ^f Cr–Cr transitions at 81 °C (18.2 kJ mol⁻¹).

upon extension of C₃H₇ to C₇H₁₅ in **4[7]c** and **4[7]j**, respectively. In addition, the chain extension in **4[3]j** lowered the T_{NI} by 18 K to 226 °C in **4[7]j**.

Binary mixtures

To assess the new materials for formulation of LCD mixtures, selected compounds were investigated as low concentration additives to nematic host **ClEster**, which is an ambient temperature nematic characterized by a small negative Δε of -0.56. In addition, solutions of 3 compounds in **CinnCN** were prepared to establish their virtual clearing temperatures [T_{NI}].



Analysis of **ClEster** solutions demonstrated that most derivatives **3[n]** and **4[n]** dissolve in the isotropic phase in concentrations up to about 10 mol%. However, solutions stable at ambient temperature for at least 24 h are limited to about 4–5 mol%. For instance, compound **4[3]c** forms stable 5.5 mol% solutions in **ClEster**. On the other hand, compound **3[5]b** and ester **4[3]g** were found to be least soluble in **ClEster**, and the latter precipitates even from a 1.3 mol% solution at ambient temperature after several hours. In contrast, **4[3]d**, the shorter analogue of **4[3]g** containing only one benzene ring, is soluble at a concentration of 3.0 mol%. Extending the alkyl chain at the thiane ring does not significantly improve solubility of the esters **4[n]** in **ClEster**. As might be expected, the most soluble compounds are those with more flexible fragments such as **4[3]i**, **4[3]j**, and **4[7]j**.

Thermal analysis of the binary mixtures established virtual N–I transition temperatures [T_{NI}] in both **ClEster** and **CinnCN** hosts by extrapolation of the mixture's N–I transition peak temperatures to pure additive (Fig. 2). Analysis of results in Table 2 demonstrates that extrapolated [T_{NI}] values are typically lower than those measured for pure compounds. This suggests phase stabilization in pure **4[n]** by dipole–dipole interactions. For instance, [T_{NI}] for pyrimidine derivative **4[3]h** is 70 K lower in **ClEster**, while for butoxyphenol **4[3]b**, [T_{NI}] is 77 K lower in **CinnCN**. The only exception is the five-ring mesogen **4[3]l** for which the extrapolated [T_{NI}] is 53 K higher than measured for the pure compound. Further analysis of the data demonstrates significant dependence of [T_{NI}] on the host for trifluorophenol derivative **4[3]d**, while for cyclohexanol ester **4[3]e** such dependence essentially is not observed.

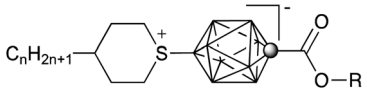
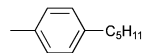
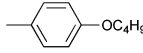
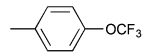
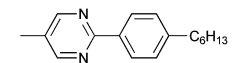
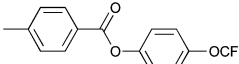
In general, three-ring esters destabilize the host's nematic phase, whereas 4- and 5-ring derivatives stabilize the host's nematic phase.

Dielectric measurements

Analysis of selected binary mixtures in **ClEster** revealed linear dependence of dielectric parameters on concentration, which, after extrapolation, established dielectric values for pure additives (Fig. 3). Analysis of the data in Table 4 demonstrates that for esters **4[5]a** and **4[3]e**, having no additional polar groups, extrapolated dielectric anisotropy, Δε, values are about 23. A lower Δε value, less than 18, was estimated for **4[3]l** on the basis of Δε < 0 for its 3 mol% solution in **ClEster**. Substituting a polar group, such as OCF₃ (in **4[3]c**) or three fluorine atoms (in **4[3]d**) into the benzene ring substantially increases the extrapolated Δε value to 70 and 60, respectively. Extension of **4[3]c** by insertion of a -C₆H₄COO- fragment (in **4[3]j**) or a -C₆H₃FCOO- fragment (in **4[3]k**) essentially does not affect the dielectric parameters of the material. Interestingly, by extending the length of the alkyl chain at the thiane



Table 3 Transition temperatures (°C) and enthalpies (kJ mol⁻¹, in italics) for 4[n]^a

				
R	n = 3	n = 5	n = 7	
a		—	Cr 97 (29.5) I ^b	—
b		Cr 111 (29.3) (N 96 (1.1)) I ^c	Cr 101 (28.6) (N 97 (0.6)) I ^b	Cr 101 (52.2) (N 93 (1.8)) I
c		Cr 135 (34.7) I	—	Cr 111 (24.6) I
h		Cr 187 (36.4) N 231 (0.7) I	Cr 187 (57.6) N 221 (2.0) I	Cr 182 (56.8) N 199 (1.3) I
j		Cr ^c 160 (23.7) N 244 (1.3) I	—	Cr 132 (36.6) N 226 (1.2) I

^a Determined by DSC (5 K min⁻¹) on heating: Cr – crystal, N – nematic, I – isotropic. ^b Ref. 5. ^c Cr–Cr transition at 137 °C (27.6); another crystalline polymorph melts at 165 °C.

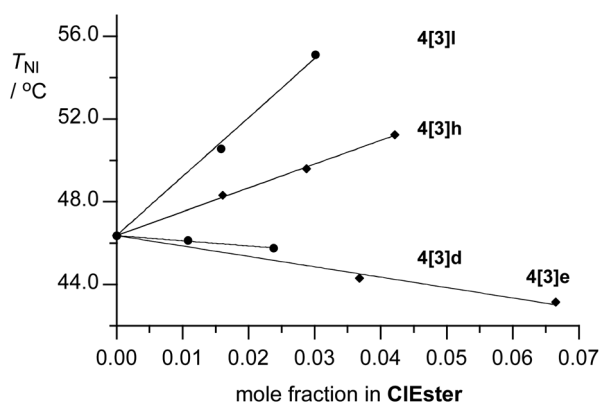


Fig. 2 Plot of peak temperatures of the N–I transition vs. concentration in ClEster.

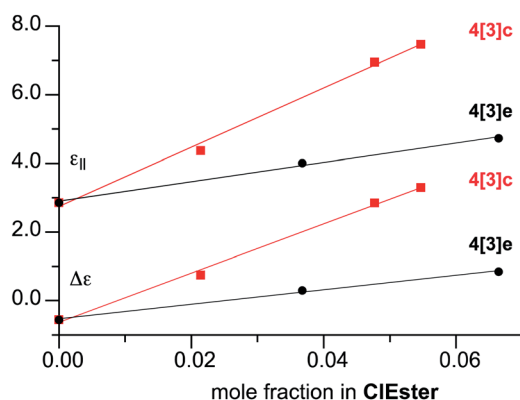


Fig. 3 Dielectric parameters of binary mixtures of 4[3]e (black) and 4[3]c (red) in ClEster as a function of concentration.

ring in the former diester (4[3]j) by $-(\text{CH}_2)_4$, $\Delta\epsilon$ increases in 4[7]j by 6%. Incorporation of the pyrimidinyl substituent as a second polar group in 4[3]h has a modest effect on dielectric anisotropy, and an extrapolated $\Delta\epsilon$ value of 50 was obtained. It appears, however, that unlike for other esters, dielectric parameters for solutions of 4[3]h deviate from linearity at higher concentrations.

Dielectric values for sulfonium 3[5]b extrapolated from two concentrations (2.5 mol% and 3.7 mol%) in ClEster are modest and about half of those previously obtained at infinite dilution for the 3[6]a analogue, which indicates significant aggregation of the additive in solutions.

Analysis of dielectric data

Dielectric parameters extrapolated for pure additives were analyzed using the Maier–Meier relationship (eqn (1)),^{18,19} which includes molecular and phase parameters.²⁰ Using experimental $\epsilon_{||}$ and $\Delta\epsilon$ values and DFT-calculated parameters μ , α , and β (Table 5), eqn (2) and (3) are used to calculate the apparent order parameter, S_{app} ,²⁰ and Kirkwood factor, g (Table 4). The effect of the additive was ignored in the determination of field parameters F and h in eqn (2) and (3); F and h were calculated using the experimental dielectric and optical data for pure ClEster host.^{21,22}

$$\Delta\epsilon = \frac{NFh}{\epsilon_0} \left\{ \Delta\alpha - \frac{F\mu_{\text{eff}}^2}{2k_B T} (1 - 3 \cos^2 \beta) \right\} S \quad (1)$$

$$S = \frac{2\Delta\epsilon\epsilon_0}{NFh[2\Delta\alpha + 3\bar{\alpha}(1 - 3 \cos^2 \beta)] - 3(\bar{\epsilon} - 1)\epsilon_0(1 - 3 \cos^2 \beta)} \quad (2)$$

$$g = \frac{\left[(\epsilon_{||} - 1)\epsilon_0 - \bar{\alpha}NFh - \frac{2}{3}\Delta\alpha NFhS \right] 3k_B T}{NF^2 h \mu^2 [1 - (1 - 3 \cos^2 \beta)S]} \quad (3)$$



Table 4 Extrapolated experimental (upper) and predicted (lower in italics) dielectric data and results of Maier–Meier analysis for selected compounds^a

Compound	$\epsilon_{ }$	ϵ_{\perp}	$\Delta\epsilon$	S_{app}	g
3[5]b	46	9	37	0.69	0.25
	84.9	15.9	69.0	0.65 ^b	0.50 ^b
3[6]a ^c	84	23	61	0.52	0.49
	95.2	18.2	77.0	0.65 ^b	0.50 ^b
4[5]a ^d	35.0	9.7	25.3	0.60	0.57
	32.6	8.2	24.4	0.65 ^b	0.50 ^b
4[3]c	87	17	70	0.62	0.77
	58.5	11.3	47.2	0.65 ^b	0.50 ^b
4[3]d	78	18	60	0.58	0.61
	68.2	13.0	55.2	0.65 ^b	0.50 ^b
4[3]e	32	11	21	0.51	0.55
	32.6	8.1	24.5	0.65 ^b	0.50 ^b
4[3]g	^e	^e	^e	—	—
	59.5	11.4	48.1	0.65 ^b	0.50 ^b
4[3]h	61	11	50	0.68	0.69
	44.1	9.3	34.8	0.65 ^b	0.50 ^b
4[3]j	86	17	69	0.62	0.73
	61.8	11.5	50.3	0.65 ^b	0.50 ^b
4[7]j	89	15	74	0.67	0.78
	56.8	10.9	45.9	0.65 ^b	0.50 ^b
4[3]k	87	16	71	0.63	0.67
	67.4	12.0	55.4	0.65 ^b	0.50 ^b
4[3]l	^f	^f	<18 ^f	—	—
	25.4	7.6	17.8	0.65 ^b	0.50 ^b
4[3]m	^e	^e	^e	—	—
	99.3	17.9	81.4	0.65 ^b	0.50 ^b

^a Values predicted for assumed $S_{app} = 0.65$ and $g = 0.5$. For details see text and the ESI. Typical error of experimental extrapolated dielectric parameters ± 1 . ^b Assumed value. ^c Experimental data from ref. 3. ^d Experimental data from ref. 5. ^e Not measured; see text. ^f $\Delta\epsilon < 0$ for a 3.0 mol% mixture.

Table 5 Calculated molecular parameters for selected compounds^a

Compound	$\mu_{ }/\text{D}$	μ_{\perp}/D	μ/D	$\beta^b/^\circ$	$\Delta\alpha/\text{\AA}^3$	$\alpha_{avg}/\text{\AA}^3$
3[5]b	16.39	2.38	16.57	8.3	36.18	62.40
3[6]a	16.10	2.95	16.37	10.4	24.84	53.34
4[3]a	10.39	2.42	10.66	13.2	36.45	61.32
4[5]a	10.30	2.96	10.72	16.1	37.50	65.05
4[3]c	13.99	1.95	14.12	7.9	32.91	53.92
4[3]d	14.66	2.16	14.81	8.4	30.49	51.54
4[3]e	9.77	2.64	10.12	15.1	27.02	56.83
4[3]g	14.77	1.90	14.89	7.1	47.60	64.19
4[3]h	12.94	2.33	13.14	10.2	57.74	75.86
4[3]j	16.15	1.68	16.24	5.9	50.23	69.08
4[7]j	16.16	2.05	16.29	7.2	52.12	76.59
4[3]k	17.16	0.67	17.18	2.2	52.73	69.77
4[3]l	10.56	4.13	11.34	21.4	61.47	89.21
4[3]m	17.18	2.25	17.33	7.5	39.14	54.86

^a Obtained at the B3LYP/6-31G(d,p) level of theory in **ClEster** dielectric medium. For esters **4[n]** calculated for an average molecule at the equilibrium ($[cis] = 21 \text{ mol\%}$). For details see text and the ESI. ^b Angle between the net dipole vector μ and $\mu_{||}$.

The molecular electric dipole moment, μ , and polarizability, α , required for the Maier–Meier analysis were obtained at the B3LYP/6-31G(d,p) level of theory in the dielectric medium of **ClEster**.²² While molecules in series **3[n]** are essentially

conformationally stable with a strong preference for the *trans* isomer in the diequatorial form,⁵ sulfonium esters **4[n]** exist as a dynamic mixture of interconverting stereoisomers *trans* and *cis* in about 4 : 1 ratio (Fig. 4).⁵ Therefore, their molecular parameters were obtained as a weighted sum of values calculated for the two stereoisomers **4[n-trans]** and **4[n-cis]** and the composite numbers for **4[n]** are shown in Table 5.²²

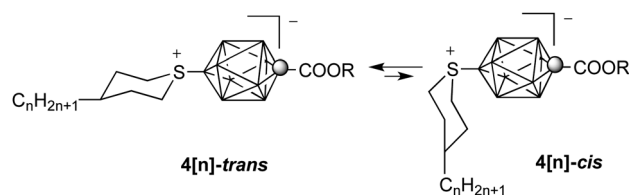
Results in Table 5 demonstrate that replacement of the pentyl chain in **3[6]a** with the 4-propylphenethyl group in **3[5]b** essentially has no effect on the molecular dipole moment ($\mu \approx 16.5 \text{ D}$), however it increases anisotropy of polarizability by about 50% from $\Delta\alpha = 24.8 \text{ \AA}^3$ in **3[6]a** to $\Delta\alpha = 36.2 \text{ \AA}^3$ in **3[5]b**.

The dipole moment of esters **4[n]** with a non-polar alcohol and phenol (e.g. **4[3]a** and **4[3]e**, Table 5) is about 6 D lower than for compounds in series **3[n]**. It can be increased by introduction of additional polar groups into the molecular structure of **4[n]**. Hence, replacement of the pentyl chain in **4[3]a** with a polar group, such as OCF_3 (**4[3]c**), 3 fluorine atoms (**4[3]d**), or CN (**4[3]m**, Chart 1) increases the longitudinal dipole moments by 3.5 D, 4.2 D and 6.7 D, respectively. Extending the molecular core in ester **4[3]d** by another benzene ring in **4[3]g** has negligible effect on the dipole moment, but it does increase anisotropy of polarizability by about 50% from $\Delta\alpha = 30.4 \text{ \AA}^3$ in the former to $\Delta\alpha = 47.6 \text{ \AA}^3$ in the latter with a modest increase in average polarizability α ($\sim 25\%$). Similar extension of **4[3]c** with a weakly polar $-\text{C}_6\text{H}_4\text{COO}-$ fragment in **4[3]j** increases the longitudinal dipole moment by 2.2 D and significantly increases $\Delta\alpha$ (53%) and α (28%). Placement of a fluorine atom on the $-\text{C}_6\text{H}_4\text{COO}-$ group in **4[3]j** further increases the dipole moment in **4[3]k** by 1 D, with a minimal impact on polarizability.

The longitudinal dipole moment in esters **4[n]** was also increased by incorporation of a pyrimidine fragment; compounds possessing such a fragment are known to exhibit substantial dielectric anisotropies.²³ Thus, the ester of 2-(4-hexylphenyl)pyrimidin-5-ol, derivative **4[3]h**, has a calculated dipole moment $\mu = 13.14 \text{ D}$, which is about 2.5 D higher than that of 4-pentylphenol **4[3]a**.

Lateral fluorination has no effect on the magnitude of the longitudinal molecular dipole moment component, $\mu_{||}$. Thus, results for **4[3]l** show that $\mu_{||}$ remains nearly the same as in the 4-pentylphenol ester **4[3]a**. However, the transverse component, μ_{\perp} , of the molecular dipole moment increases by 1.7 D, changing the orientation of the net dipole moment vector with respect to the main molecular axis from $\beta = 13.1^\circ$ in **4[3]a** to $\beta = 21.3^\circ$ in **4[3]l**.

Analysis of the computational results for the **4[3-trans]** isomers shows that, with the exception of **4[3]l**, the net dipole moment is nearly parallel with the long molecular axis, and the

**Fig. 4** Interconversion of the *trans* and *cis* isomers of ester **4[n]**.

angle β ranges from 2° in **4[3]k** to 14° in **4[3]e** (avg. $7.8^\circ \pm 3.7^\circ$). In the **4[3]-cis** isomers the angle β is larger by an average of $4.6^\circ \pm 1.7^\circ$ relative to the *trans* analogues. The molecular shape also affects anisotropy of polarizability $\Delta\alpha$, which is larger for the linear **4[3]-trans** molecules than for the bent **4[n]-cis** analogues by an average of $4.6 \pm 0.5 \text{ \AA}^3$.

The effectiveness of these compounds as high $\Delta\epsilon$ additives to **ClEster** was investigated using the Maier–Meier formalism. Following a frequently used approach in designing of polar liquid crystals, the analysis initially assumed the order parameter of the additives to be the same as for the **ClEster** host ($S = 0.65$), and Kirkwood factor (g) was set at 0.5.^{24,25} Results in Table 4 demonstrate that esters **4[n]** of non-polar phenols or alcohols exhibit expected $\Delta\epsilon$ values of about 24 (**4[5]a** and **4[3]e**). The lowest $\Delta\epsilon$ value of 17.8 is predicted for **4[3]l**, which is the largest molecule investigated in this series. This low value is due, in part, to the low number of molecules in the unit volume (low N number).

Esters of phenols with polar substituents are expected to have higher $\Delta\epsilon$ values. Thus, OCF_3 , F, and additional COO groups enhance the longitudinal dipole moment, which results in $\Delta\epsilon$ of about 50 (e.g. **4[3]c**, **4[3]d**, and **4[3]j**). A particularly large $\Delta\epsilon$ of 81 is predicted for ester **4[3]m** containing a CN group (Chart 1). Surprisingly, the least effective dipole moment booster is the pyrimidine fragment in **4[3]h**, with a predicted relatively low $\Delta\epsilon$ of 35.

Compounds in series **3[n]** have predicted higher $\Delta\epsilon$ values (~ 70) than those for esters **4[n]**. However, these values are observed only at infinitely low concentrations. At higher concentration ($\sim 2 \text{ mol\%}$) molecular aggregation significantly reduces $\Delta\epsilon$.

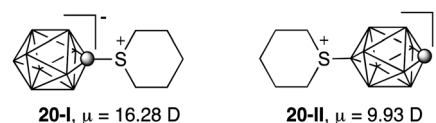
Experimental $\Delta\epsilon$ for **4[n]** are in general agreement with theoretical predictions, mainly due to fairly high and uniform S_{app} values. Analysis of data in Table 4 demonstrates that experimental S_{app} of 0.61 ± 0.02 for the compounds are comparable with the order parameter of **ClEster** ($S = 0.65$). The only exceptions are **4[3]e** ($S_{\text{app}} = 0.51$), **4[3]h** ($S_{\text{app}} = 0.68$), and **4[7]j** ($S_{\text{app}} = 0.67$). These outlying S_{app} values for the first two compounds are consistent with the extreme virtual clearing temperatures, $[T_{\text{NI}}] = -4^\circ\text{C}$ for **4[3]e** and $[T_{\text{NI}}] = 161^\circ\text{C}$ for **4[3]h**, and demonstrate low compatibility of the former (**4[3]e**) and higher compatibility of the latter (**4[3]h**) with the host.

The Kirkwood parameter, g , has a broader range for esters **4[n]** between 0.55 for **4[3]e** and 0.78 for **4[7]j** and reflects different degrees of molecular association of the additive in solutions. In general, the observed values for g are higher than that initially assumed ($g = 0.5$). Perhaps most gratifying is that compounds **4[3]j**, **4[7]j**, and **4[3]k** with the highest values of $\mu_{||}$ show little association ($g = 0.73$, 0.78 , and 0.67 , respectively). Particularly interesting is the observed decreased association (increased g) upon alkyl chain extension in **4[n]j**. This demonstrates that molecular structure containing several polar groups placed in the semi-rigid core provide a successful design for preparation of high $\Delta\epsilon$ materials. On the other hand, analysis of compounds in series **3[n]** gives low g values (e.g. $g = 0.25$ for **3[5]b**), which shows that these materials are prone to excessive aggregation in solutions. This is also consistent with

their low solubility and non-linear dependence of dielectric parameters *versus* concentration.

Discussion

The centerpiece of polar materials presented here is the sulfonium zwitterion **20** of the $[\text{closo-1-CB}_9\text{H}_{10}]^-$ cluster with calculated ground-state electric dipoles of 16.3 D and 9.9 D for zwitterions **20-I** and **20-II**, respectively, in **ClEster** dielectric medium. The observed difference in the dipole moments originates from the strong polarization of electron density towards the carbon atom in the boron cluster. Elongation of the molecular core by substitution in the antipodal positions of the $[\text{closo-1-CB}_9\text{H}_{10}]^-$ cluster and the thiane ring in **20-I** and **20-II** helps to induce liquid crystalline behavior and increases compatibility with nematic hosts. In general, compounds with a total of 2 or 3 rings in both series **3[n]** and **4[n]** do not form liquid crystalline phases; the only exception thus far is the 4-butoxyphenol ester **4[n]b**.



The calculated longitudinal dipole moment, $\mu_{||}$, in compounds **3[n]** is about 16 D and originates solely from **20-I**. Esters **4[n]** can achieve the same magnitude of $\mu_{||}$ by combining the moderate dipole moment of **20-II** with that of a polar substituent. Examples include diesters **4[n]j** and benzonitrile **4[3]m**, in which the net dipole moments are calculated to be 16.2 and 17.3 D, respectively (Table 5). In contrast to **3[n]**, compounds **4[n]** with several polar groups exhibit lower melting points, higher solubility in nematic hosts, and display mesogenic behavior. These qualities are quantified in the Maier–Meier analysis and reflected in high order, S_{app} , and Kirkwood, g , parameters, as shown for diesters **4[n]j** and **4[3]k** (Table 4).

Results in Table 4 indicate that small polar compounds are more effective additives due to their higher density of dipoles in the unit volume (larger number density N). For instance, ester **4[3]c** and its “extended” analogue diester **4[3]j** have essentially the same experimental dielectric parameters ($\Delta\epsilon \approx 70$) in spite of a larger dipole moment in the latter by about 2 D (Table 5). Benzonitrile derivative **4[3]m**, although not prepared in this investigation, is expected to exhibit a relatively large dielectric anisotropy, on the basis of its small size and large dipole moment.

Finally, it should be emphasized that analysis of experimental dielectric data using the Maier–Meier formalism provides informative insight into the behavior of additives in nematic solutions and has become an important tool in our investigation of polar compounds.²⁰

Conclusions

We have reported a diverse library of two series of polar compounds derived from an inorganic boron cluster, which act



as effective additives to nematic materials for modulating dielectric anisotropy, $\Delta\epsilon$, and hence electrooptical properties. Compounds **3[n]** do not display liquid crystalline behavior or enhanced solubility even with elongated molecular cores up to 3 rings. However, they have high extrapolated $\Delta\epsilon$ values, but are hampered by limited solubility in nematic materials. On the other hand, esters **4[n]** have significantly improved compatibility with nematic hosts and exhibit liquid crystalline behavior. However, compounds with a total of 2 or 3 rings in **4[n]** generally do not form liquid crystalline phases. Esters **4[n]** have more modest extrapolated $\Delta\epsilon$ values due to smaller zwitterion's dipole moment, but incorporation of additional polar substituents into the molecular structure can increase $\Delta\epsilon$ values, while maintaining solubility on the order of several mol%. The most effective additives for increasing $\Delta\epsilon$ of **ClEster** appear to be **4[3]c** and **4[n]j**. These materials exhibit good compatibility with the host (reasonable solubility, high g and S_{app} values) and a large $\Delta\epsilon$ of about 70.

Additional structure–property relationship studies are needed to further increase compatibility of these polar compounds with nematic hosts. Enhanced solubility would make these classes of compounds, especially esters **4[n]**, more useful as additives in formulation of LCD mixtures.

Computational details

Quantum-mechanical calculations were carried out using Gaussian 09 suite of programs.²⁶ Geometry optimizations for unconstrained conformers of **3[5]b**, **3[6]a**, and **4[n]** with the most extended molecular shapes were undertaken at the B3LYP/6-31G(d,p) level of theory using default convergence limits. Dipole moments and exact electronic polarizabilities for **3[5]b**, **3[6]a**, and **4[n]** for analysis with the Maier–Meier relationship were obtained in **ClEster** dielectric medium using the B3LYP/6-31G(d,p)//B3LYP/6-31G(d,p) method and the PCM solvation model²⁷ requested with the SCRF (solvent = generic, read) keyword and “eps = 3.07” and “epsinf = 2.286” parameters (single point calculations). The reported values for dipole moment components and dielectric permittivity tensors are at Gaussian standard orientation of each molecule (charge based), which is close to the principal moment of inertia coordinates (mass based).

Experimental part

General

NMR spectra were obtained at 128 MHz (¹³B), 100 MHz (¹³C), and 400 MHz (¹H) in CDCl₃ or CD₃CN. Chemical shifts were referenced to the solvent (¹H, ¹³C) or to an external sample of B(OH)₃ in MeOH (¹B, δ = 18.1 ppm). Optical microscopy and phase identification were performed using a PZO “Biopolar” polarized microscope equipped with a HCS400 Instec hot stage. Thermal analysis was obtained using a TA Instruments 2920 DSC. Transition temperatures and enthalpies were typically obtained using small samples (~0.5 mg) and a heating rate of 5 K min^{−1}.

Preparation of **3[n]**

A solution of anhydrous ZnCl₂ (12 eq.) in dry THF (10 mL), was treated with a solution of C_nH_{2n+1}MgBr (12 eq., 2 M in Et₂O or freshly prepared from C_nH_{2n+1}Br in THF) at 0 °C under N₂ atmosphere. The mixture was stirred for 15 min at rt, and NMP was added (5 mL) followed by Pd₂dba₃ (2 mol%), [HPCy₃]⁺[BF₄][−] (8 mol%), and iodide **6** (ref. 7) (1.0 mmol). The mixture was stirred overnight at rt, 10% HCl was added, and the mixture was extracted with Et₂O (3×). The combined extracts were dried (Na₂SO₄), and the solvent was evaporated. The resulting residue was purified by passage through a silica gel plug (hexane–CH₂Cl₂, 1 : 1). The eluent was filtered through a cotton plug, and the solvent evaporated to give the desired product in about 90% yield. Pure product for analysis was obtained by triple recrystallization (toluene–*iso*-octane) as white crystals.

Analytical data for compounds **3[n]** are provided in the ESI.†

Preparation of esters **4[n]**

Method A. A suspension of sulfonium acid **9[n]** (0.16 mmol) in CH₂Cl₂ (1 mL) was treated with (COCl)₂ (3 eq.) and anhydrous DMF (cat. amount). The suspension was stirred vigorously at rt until it became homogeneous (~30 min). The light yellow solution was then evaporated to dryness, and the residue was redissolved in anhydrous CH₂Cl₂ (1 mL). Phenol **10** (1.1 eq.) and freshly distilled NEt₃ (3 eq.) were added, and the mixture was stirred overnight at rt. The reaction mixture was washed with 5% HCl (3×), and the organic layer was dried (Na₂SO₄) and solvent removed. The product was purified by passage through a silica gel plug (CH₂Cl₂). The eluent was filtered through a cotton plug, and the solvent evaporated to give the desired ester in about 60% yield. The resulting ester was purified further by repeated recrystallization typically from an *iso*-octane–toluene mixture.

Method B. The crude acid chloride (generated from **9[3]** as in Method A), excess alcohol **11** (5 eq.), and freshly distilled pyridine (5 eq.) were stirred and heated for 3 days at 90 °C, with protection from moisture. At times, the reaction was cooled to rt, and minimal amount of anhydrous CH₂Cl₂ was added to wash the sides of the flask. The product was purified as in Method A.

Analytical data for esters **4[n]** and synthetic procedures for intermediates are provided in the ESI.†

Binary mixtures

Preparation and analysis. Solutions of compounds **3[n]** or **4[n]** and host **ClEster** (10–15 mg of the host) in dry CH₂Cl₂ (~0.5 mL) were heated at ~60 °C for 2 h in an open vial to assure homogeneity of the sample. The sample was degassed under vacuum (0.2 mmHg), left at ambient temperature for 2 h, and analyzed by polarized optical microscopy (POM). Homogeneous samples were used for thermal and dielectric measurements. Long-term stability of the solutions was determined by analyzing the samples by POM after at least 20 h at ambient temperature.

The clearing temperature for each homogeneous mixture was determined by DSC as the peak of the transition using small



samples (~ 0.5 mg) and a heating rate of 5 K min^{-1} . The results are provided in the ESI. The virtual N–I transition temperatures, $[T_{\text{NI}}]$, were determined by linear extrapolation of the data for the peak of the transition to pure substance ($x = 1$). To minimize the error, the intercept in the fitting function was set as the peak T_{NI} for the pure host.

Electrooptical measurements. Dielectric properties of solutions of selected esters in **ClEster** were measured by a Liquid Crystal Analytical System (LCAS – Series II, LC Vision, Inc.) using GLCAS software version 0.13.14, which implements literature procedures for dielectric constants.²⁸ The instrument was calibrated using a series of capacitors. The homogeneous binary mixtures were loaded into ITO electro-optical cells by capillary forces with moderate heating supplied by a heat gun. The cells (about $10\text{ }\mu\text{m}$ thick, electrode area 1.00 cm^2 and anti-parallel rubbed polyimide layer) were obtained from LC Vision, Inc. The filled cells were heated to the isotropic phase and cooled to rt before measuring the dielectric properties. Default parameters were used for measurements: triangular shaped voltage bias ranging from $0.1\text{--}20\text{ V}$ at 1 kHz frequency. The threshold voltage, V_{th} , was measured at a 5% change. For each mixture the measurement was repeated 10 times for two cells. The results were averaged to calculate the mixture's dielectric parameters. Results are provided in the ESI† and extrapolated values for pure additives are shown in Table 4.

Acknowledgements

This work was supported by NSF grant DMR-1207585. We are grateful to Professor Roman Dąbrowski of the Military University of Technology (Warsaw, Poland) for the gift of **ClEster**.

References

- 1 D. Pauluth and K. Tarumi, *J. Mater. Chem.*, 2004, **14**, 1219–1227.
- 2 M. Bremer, P. Kirsch, M. Klasen-Memmer and K. Tarumi, *Angew. Chem., Int. Ed.*, 2013, **52**, 8880–8896.
- 3 B. Ringstrand, P. Kaszynski, A. Januszko and V. G. Young, Jr, *J. Mater. Chem.*, 2009, **19**, 9204–9212.
- 4 J. Pecyna, D. Pociecha and P. Kaszyński, *J. Mater. Chem. C*, 2014, **2**, 1585–1591.
- 5 B. Ringstrand and P. Kaszynski, *J. Mater. Chem.*, 2011, **21**, 90–95.
- 6 B. Ringstrand and P. Kaszynski, *J. Mater. Chem.*, 2010, **20**, 9613–9615.
- 7 B. Ringstrand, M. Oltmanns, J. A. Batt, A. Jankowiak, R. P. Denicola and P. Kaszynski, *Beilstein J. Org. Chem.*, 2011, **7**, 386–393.
- 8 J. Pecyna, R. P. Denicola, B. Ringstrand, A. Jankowiak and P. Kaszynski, *Polyhedron*, 2011, **30**, 2505–2513.
- 9 B. Ringstrand, P. Kaszynski, V. G. Young, Jr and Z. Janoušek, *Inorg. Chem.*, 2010, **49**, 1166–1179.
- 10 J. Thomas and D. Clough, *J. Pharm. Pharmacol.*, 1963, **15**, 167–177.
- 11 N. Aziz, S. M. Kelly, W. Duffy and M. Goulding, *Liq. Cryst.*, 2008, **35**, 1279–1292.
- 12 J. Qiu, L. Wang, M. Liu, Q. Shen and J. Tang, *Tetrahedron Lett.*, 2011, **52**, 6489–6491.
- 13 T. A. Kizner, M. A. Mikhaleva and E. S. Serebryakova, *Chem. Heterocycl. Compd.*, 1990, **26**, 668–670.
- 14 B. Ringstrand, A. Jankowiak, L. E. Johnson, P. Kaszynski, D. Pociecha and E. Górecka, *J. Mater. Chem.*, 2012, **22**, 4874–4880.
- 15 S. M. Kelly, *Helv. Chim. Acta*, 1989, **72**, 594–607.
- 16 A. Jankowiak, B. Ringstrand, A. Januszko, P. Kaszynski and M. D. Wand, *Liq. Cryst.*, 2013, **40**, 605–615.
- 17 S. Hayashi, S. Takenaka and S. Kusabayashi, *Bull. Chem. Soc. Jpn.*, 1984, **57**, 283–284.
- 18 W. Maier and G. Meier, *Z. Naturforsch., A: Phys. Sci.*, 1961, **16**, 262–267 and 470–477.
- 19 S. Urban, in *Physical Properties of Liquid Crystals: Nematics*, ed. D. A. Dunmur, A. Fukuda and G. R. Luckhurst, IEE, London, 2001, pp. 267–276.
- 20 P. Kaszyński, A. Januszko and K. L. Glab, *J. Phys. Chem. B*, 2014, **118**, 2238–2248.
- 21 R. Dabrowski, J. Jadzyn, S. Czerkas, J. Dziaduszek and A. Walczak, *Mol. Cryst. Liq. Cryst.*, 1999, **332**, 61–68.
- 22 For details see the ESI.†
- 23 A. I. Pavluchenko, N. I. Smirnova, V. F. Petrov, Y. A. Fialkov, S. V. Shelyazhenko and L. M. Yagupolsky, *Mol. Cryst. Liq. Cryst.*, 1991, **209**, 225–235.
- 24 P. Kędziora and J. Jadzyn, *Mol. Cryst. Liq. Cryst.*, 1990, **192**, 31–37.
- 25 P. Kędziora and J. Jadzyn, *Acta Phys. Pol., A*, 1990, **77**, 605–610.
- 26 M. J. Frisch, G. W. Trucks, H. B. Schlegel, G. E. Scuseria, M. A. Robb, J. R. Cheeseman, G. Scalmani, V. Barone, B. Mennucci, G. A. Petersson, H. Nakatsuji, M. Caricato, X. Li, H. P. Hratchian, A. F. Izmaylov, J. Bloino, G. Zheng, J. L. Sonnenberg, M. Hada, M. Ehara, K. Toyota, R. Fukuda, J. Hasegawa, M. Ishida, T. Nakajima, Y. Honda, O. Kitao, H. Nakai, T. Vreven, J. A. Montgomery, Jr, J. E. Peralta, F. Ogliaro, M. Bearpark, J. J. Heyd, E. Brothers, K. N. Kudin, V. N. Staroverov, R. Kobayashi, J. Normand, K. Raghavachari, A. Rendell, J. C. Burant, S. S. Iyengar, J. Tomasi, M. Cossi, N. Rega, J. M. Millam, M. Klene, J. E. Knox, J. B. Cross, V. Bakken, C. Adamo, J. Jaramillo, R. Gomperts, R. E. Stratmann, O. Yazyev, A. J. Austin, R. Cammi, C. Pomelli, J. W. Ochterski, R. L. Martin, K. Morokuma, V. G. Zakrzewski, G. A. Voth, P. Salvador, J. J. Dannenberg, S. Dapprich, A. D. Daniels, O. Farkas, J. B. Foresman, J. V. Ortiz, J. Cioslowski and D. J. Fox, *Gaussian 09, Revision A.02*, Gaussian, Inc., Wallingford CT, 2009.
- 27 M. Cossi, G. Scalmani, N. Rega and V. Barone, *J. Chem. Phys.*, 2002, **117**, 43–54 and references therein.
- 28 S.-T. Wu, D. Coates and E. Bartmann, *Liq. Cryst.*, 1991, **10**, 635–646.

